INSTITUT D'AERONOMIE SPATIALE DE BELGIQUE

3 - Avenue Circulaire
B - 1180 BRUXELLES

AERONOMICA ACTA

A - N° 162 - 1976

The plasmapause as a plasma sheath: a minimum thickness

by

M. ROTH

BELGISCH INSTITUUT VOOR RUIMTE-AERONOMIE

3 - Ringlaan
B - 1180 BRUSSEL

FOREWORD

The paper "The plasmapause as a plasma sheath : a minimum thickness" will be published in Journal of Atmospheric and Terrestrial Physics.

AVANT-PROPOS

L'article "The plasmapause as a plasma sheath : a minimum thickness" sera publié dans Journal of Atmospheric and Terrestrial Physics.

VOORWOORD

De tekst "The plasmapause as a plasma sheath : a minimum thickness" zal gepubliceerd worden in Journal of Atmospheric and Terrestrial Physics.

VORWORT

Der Text "The plasmapause as a plasma sheath : a minimum thickness" wird in Journal of Atmospheric and Terrestrial Physics herausgegeben werden.

THE PLASMAPAUSE AS A PLASMA SHEATH : A MINIMUM THICKNESS

by

M. ROTH

Abstract

We consider the plasmapause as a stationary boundary layer (a sheath) separating two types of plasmas characterized by different temperatures and densities : on one side, the hot trapped particles imbedded in the cold exospheric plasma of ionospheric origin, and on the other side the plasmatrough including the hot ring current particles. The structure of this layer is described by a kinetic model using the Vlasov-Maxwell's equations for the charged particles and fields. In absence of any collisional effects or wave-particle interactions a minimum value for the thickness of the plasmapause is deduced which is of the order of 5 times the Larmor radius of the cold ions.

Résumé

Nous considérons la plasmapause comme une couche frontière stationnaire (une gaîne) séparant deux types de plasmas caractérisés par des températures et des densités différentes : d'un côté, remplissant l'exosphère, les particules énergétiques piègées, encastrées dans le plasma thermique d'origine ionosphérique; de l'autre côté, le plasma de la "trough" comprenant les particules énergétiques du courant annulaire. La structure de cette couche est décrite par un modèle cinétique basé sur les équations de Vlasov-Maxwell qui régissent, de manière auto-consistante, l'évolution des fonctions de distribution des particules chargées et la description des champs électromagnétiques. En l'absence d'effet collisionnel ou d'interactions ondes-particules, on déduit une valeur minimum de l'épaisseur de la plasmapause. Cette valeur est de l'ordre de 5 fois le rayon de Larmor des ions thermiques.

Samenvatting

We beschouwen de plasmapause als een stationaire grenslaag tussen twee soorten plasma's gekenmerkt door verschillende temperaturen en dichtheden : enerzijds heeft men energetische deeltjes gevat in het thermisch plasma van ionosferische oorsprong, anderzijds heeft men de "plasma-trough" die de energetische deeltjes van de ringstroom omvat. De struktuur van deze laag wordt beschreven door een kinetisch model. Er wordt daarbij gebruik gemaakt van de vergelijkingen van Vlasov-Maxwell voor geladen deeltjes en velden. Bij afwezigheid van botsingseffekten of interakties tussen golven en deeltjes, kan men een minimumwaarde afleiden voor de dikte van de plasmapause. De grootte-orde van die minimumwaarde bedraagt vijf maal de Larmor straal van de thermische ionen.

Zusammenfassung

Wir betrachten hier die Plasmapause als eine stationäre Grenzenschicht die zwei verschiedene Plasmas trennt : einerseits is der exosphären Plasma und auf der anderen Seite liegt der Plasmatrough Plasma mit seine "Ring Current" Teilchen. Die Strucktur dieser Schicht ist durch ein kinetisches Model mit Vlasov-Maxwell Gleichungen beschrieben worden. Die Rechnungen geben ein minimale Schichten Breite von 5 mal das Larmor Radius der kalten Ionen, an.

I. INTRODUCTION

We define the plasmapause as a boundary layer separating two regions, the plasmasphere and the plasmatrough, each of which having distinctly different properties. Cold plasma of approximately 1 eV evaporated from the top of the ionosphere is the main constituent of the plasmasphere. In the plasmatrough, hot ring current particles with characteristic energy 0.1 - 50 keV, of magnetospheric origin, become the dominant particles.

The purpose of this paper is to present a microscopic and basic description of the structure of this boundary. It is assumed that a change in the macroscopic velocity occurs across the plasma sheath : the plasmasphere corotates with the Earth, while the plasmatrough has a larger drift velocity. For describing the structure of this sheath we use a model based on an extension of the work of Sestero (1964, 1966) on contact discontinuities in collisionless plasmas. This model is described in Section 2. Boundary conditions on each side of the plasmapause are described in Section 3. In Section 4, these boundary conditions are used to calculate some characteristic lengths and velocities, and to determine numerically the variations of the most important physical parameters through the transition. Conclusions are summarized in Section 5.

II. DESCRIPTION OF THE MODEL

Figure 1 represents the geometry of the model. It is a local representation of the plasmapause in the night-side sector. The x-y plane is the plane of the earth equator and the y-z plane represents the boundary surface. We make the assumption of steady-state and we assume that every physical quantity depends on one space coordinate, the x coordinate. The magnetic field $\vec{B}$ points along the z-axis while the electric field $\vec{E}$ is directed along the x-axis. The current $\vec{J}$ and the vector potential $\vec{a}$ are in the y-direction. The plasma moves in the y-direction with different velocities on both sides of the boundary layer. In the plasmasphere and plasmatrough regions, far enough from the plasmapause, the plasma is assumed to be uniform and Maxwellian. The macroscopic velocities are denoted by $\vec{V}_1$ in the plasmasphere and by $\vec{V}_2$ in the plasmatrough. Cold and hot plasmas contain only hydrogen ions.

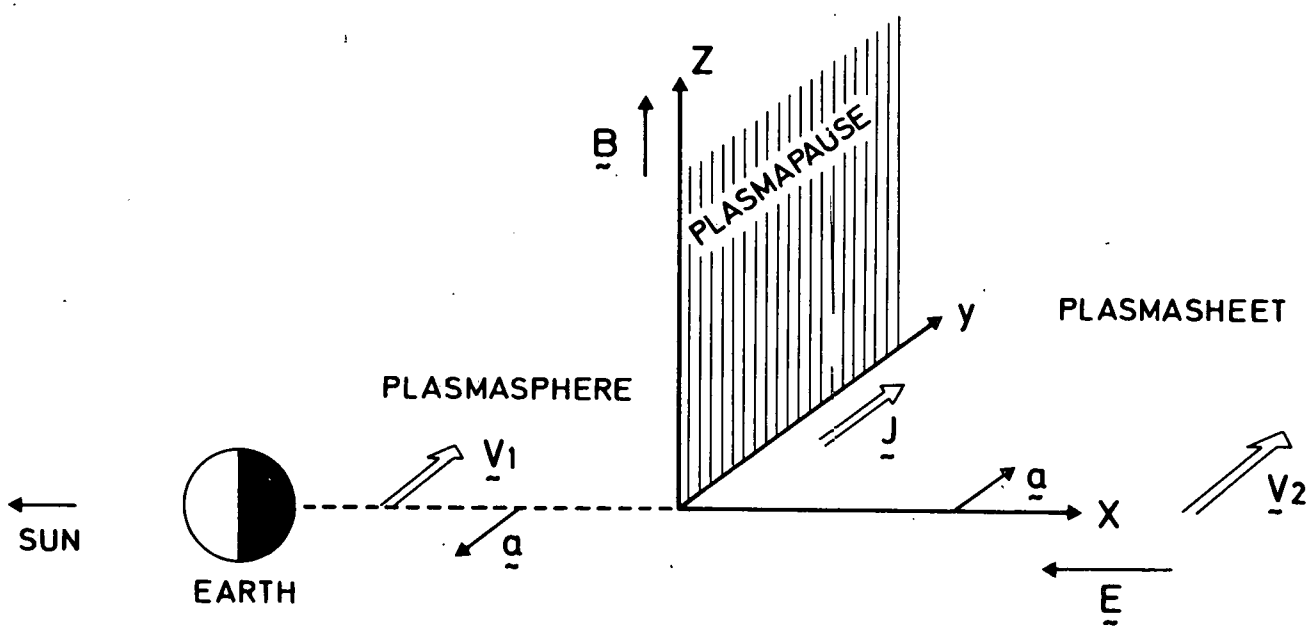

Fig. 1.- Geometry of the model.

A microscopic description of this sheath is made by using Vlasov's equation for the distribution functions of the charged particles coupled with the Maxwell's equations for the electromagnetic fields. Any function of the constants of motion is a solution of Vlasov's equation. The constants of motion are the total energy and the generalized momentum p along the y-axis :

$$\epsilon = \frac{1}{2} m_{\pm} (u^2 + v^2) \pm e\,\phi(x) \qquad (1)$$

$$p = m_{\pm} v \pm ea(x) \qquad (2)$$

The subscripts + and - are respectively for ions and electrons. Here u and v are the components of velocities along the x and y axies, e is the charge of the proton, $m_{\pm}$ are the masses of the charged particles, $\vec{a}$ and ϕ are the magnetic vector potential and the scalar electric potential satisfying Maxwell's equations :

$$\frac{1}{\mu} \frac{d^2 a}{dx^2} = -J \qquad (3)$$

$$\kappa \frac{d^2 \phi}{dx^2} = -q \qquad (4)$$

$\vec{J}$ and q are the current and charge densities, κ and μ being the permittivity and permeability of the vacuum in rationalized M.K.S. units.

In the situation considered here, we have a mixture of cold and hot non-collisionless plasmas interacting in the transition layer separating two uniform regions with distinctly different properties and including a change in the macroscopic velocity of the two regions. The simplest model describing such a transition (Sestero, 1964, 1966) uses, for each type of plasma, distribution functions for the charged particles $F^i_{\pm}(p, \epsilon)$, which are the sum of two different displaced Maxwellians (the superscripts i denotes the cold (c) or the hot (h) plasma) :

$$F^i_{\pm}(p,\epsilon) = F^i_{1\pm}(p,\epsilon) + F^i_{2\pm}(p,\epsilon) \qquad (5)$$

with

$$F^i_{1\pm}(p,\epsilon) =$$

$$\begin{cases} \dfrac{N^i_{\pm}\, m_{\pm}}{2\pi\, kT^i_{1\pm}} \cdot \exp\left(-\dfrac{m_{\pm}\, V_1^2}{2k\, T^i_{1\pm}}\right) \cdot \exp\left(\dfrac{V_1\, p}{k\, T^i_{1\pm}}\right) \cdot \exp\left(-\dfrac{\epsilon}{kT^i_{1\pm}}\right) & \\ \qquad\qquad \text{for } p \text{ in }]\mp\infty,\ m_{\pm}\, V_1\,[& \\ 0 \qquad\qquad \text{for } p \text{ in }]\, m_{\pm}\, V_1\ ,\pm\infty\,[& \end{cases}$$

$$F^i_{2\pm}(p,\epsilon) =$$

$$\begin{cases} 0 \qquad\qquad \text{for } p \text{ in }]\mp\infty,\ m_{\pm}\, V_2\,[& \\ \dfrac{C^i_{\pm}\, N^i_{\pm}\, m_{\pm}}{2\pi\, kT^i_{2\pm}} \cdot \exp\left(-\dfrac{m_{\pm}\, V_2^2}{2kT^i_{2\pm}}\right) \cdot \exp\left(\dfrac{V_2\, p}{kT^i_{2\pm}}\right) \cdot \exp\left(-\dfrac{\epsilon}{kT^i_{2\pm}}\right) & \\ \qquad\qquad \text{for } p \text{ in }]\, m_{\pm}\ V_2\ ,\pm\infty\,[& \end{cases}$$

For each type (i) of plasma, $T^i_{1\pm}$ and $N^i_{\pm}$ are the temperatures and densities of the corresponding species in the plasmasphere, $T^i_{2\pm}$ are the temperatures in the plasmatrough. The quantities $C^i_{\pm}$ are constants ($C^i_{\pm} > 0$) related to the densities and temperatures in the plasmatrough and to the electric potential difference $[\phi - aV]^{+\infty}_{-\infty}$ through the sheath. As the magnetic field remains always positive, it is seen that the distribution functions of the ions and electrons possess the desired asymptotic properties. Indeed, when x goes to $-\infty$, the vector potential acquires large negative values; therefore, the contribution of $F^i_{1\pm}$ becomes predominant while the contribution of $F^i_{2\pm}$ tends to zero. It follows that the velocity

distributions of the plasma approach asymptotically the displaced Maxwellians given by the non-vanishing parts of $F^i_{1\pm}$. (When x goes to $+\infty$, the same argument holds by interverting the subscripts 1 and 2, the vector potential taking large positive values).

However, the state of the plasma at both ends of the transition region does not uniquely determine the transition profile (Sestero, 1964, 1966). In the sheath, the particular forms of the distribution functions determine only the shape of the transition. The solutions of the Vlasov's equation used here correspond to one among many other possible solutions satisfying the same conditions at infinity, i.e., deep in the plasmasphere and plasmatrough regions.

The concentrations $n^i_\pm(x)$ and the current densities $J^i_\pm(x)$ can be analytically determined by evaluating moments of the distribution functions. In dimensionless variables, denoted with stars, we find :

$$n^{*i}_\pm = \rho^i_\pm \exp[\mp a^i_{1\pm}(\phi^* - 2V^*_1 a^*)] \cdot [1 - \mathrm{erf}(a^{i\ 1/2}_{1\pm}\ \gamma_\pm a^*)] + C^i_\pm \rho^i_\pm \exp[\mp a^i_{2\pm}(\phi^* - 2V^*_2 a^*)] \cdot \mathrm{erf}(a^{i\ 1/2}_{2\pm}\ \gamma_\pm a^*) \quad (6)$$

$$J^{*i}_\pm = \rho^i_\pm \exp[\mp a^i_{1\pm}(\phi^* - 2V^*_1 a^*)] \cdot \left\{ \pm V^*_1 [1 - \mathrm{erf}(a^{i\ 1/2}_{1\pm}\ \gamma_\pm a^*)] - \frac{\gamma_\pm}{2(\pi a^i_{1\pm})^{1/2}} \exp(-a^i_{1\pm}\gamma^2_\pm a^{*2}) \right\} + C^i_\pm \rho^i_\pm \exp[\mp a^i_{2\pm}(\phi^* - 2V^*_2 a^*)] \cdot \left\{ \pm V^*_2 \mathrm{erf}(a^{i\ 1/2}_{2\pm}\ \gamma_\pm a^*) + \frac{\gamma_\pm}{2(\pi a^i_{2\pm})^{1/2}} \exp(-a^i_{2\pm}\gamma^2_\pm a^{*2}) \right\} \quad (7)$$

where the error function is defined by : $\mathrm{erf}(x) = \frac{1}{\pi^{1/2}} \int_{-\infty}^{x} e^{-t^2} dt$. The following relations hold :

$$n_{\pm}^{*i}\ (x^*) = n_{\pm}^{i}\ (x) / N_{-}^{c}$$

$$J_{\pm}^{*i}\ (x^*) = \left[\left(\frac{m_{-}}{2kT_{1-}^{1}} \right)^{1/2} / eN_{-}^{c} \right] J_{\pm}^{i}\ (x)$$

$$x^* = e \left(\frac{\mu N_{-}^{c}}{m_{-}} \right)^{1/2} x$$

$$\rho_{\pm}^{i} = N_{\pm}^{i} / N_{-}^{c}$$

$$n_{j\pm}^{i} = T_{1-}^{c} / T_{j\pm}^{i}\ , j = 1, 2$$

$$\phi^* = e\phi / k\ T_{1-}^{c}$$

$$V_j^* = \left(\frac{m_{-}}{2kT_{1-}^{c}} \right)^{1/2} V_j\ ,\ j = 1, 2$$

$$a^* = (e^2 / 2m_{-}\ k\ T_{1-}^{c})^{1/2}\ a$$

$$\gamma_{\pm} = \left(\frac{m_{\pm}}{m_{+}} \right)^{1/2}$$

For the charge densities $q_{\pm}^{i}$, we have :

$$q_{\pm}^{*i} = q_{\pm}^{i} / e\ N_{-}^{c}\ ,\ \text{so that}\ n_{\pm}^{*i} = \pm\ q_{\pm}^{*i}$$

One can also deduces the following relations for the fields :

$$E^* = \frac{1}{kT_{1-}^{c}} \left(\frac{m_{-}}{\mu N_{-}^{c}} \right)^{1/2} E$$

$$B^* = (2\mu\ N_-^c\ k\ T_{1-}^c)^{-1/2}\ B$$

The basic equations (3) and (4) become in dimensionless form :

$$\begin{cases} \dfrac{d^2 a^*}{dx^{*2}} = -J^* & (8) \\ \dfrac{\kappa\ \mu\ k\ T_{1-}^c}{m_-} \dfrac{d^2\phi^*}{dx^{*2}} = -q^* & (9) \end{cases}$$

These equations can be integrated numerically to determine the distribution of the vector and electric potentials. The total current J^* is the sum : $J_+^{*c} + J_-^{*c} + J_+^{*h} + J_-^{*h}$ of the partial current densities due to the cold (c) and hot (h) ions and electrons. At this point, however, it is suitable to make the simplifying approximation of charge-neutrality. This approximation replaces the Poisson's equation (9) for the electric potential by the algebraic equation of charge neutrality everywhere, i.e.,

$$q^* = q_+^{*c} + q_-^{*c} + q_+^{*h} + q_-^{*h} = 0. \qquad (10)$$

The small quantity $\dfrac{\kappa\ \mu\ kT_{1-}^c}{m_-}$ is the square of the ratio of the mean thermal speed of the cold electrons of the plasmasphere to the speed of light. For a typical value of 1 eV for $k\ T_{1-}^c$, this quantity is equal to 1.95×10^{-6}. It is expected, therefore, that, with a electric potential solution of (10), the first member of equation (9) remains everywhere a small quantity, so that this potential is self-consistent. In the section IV, it will indeed be shown, that the charge neutral approximation holds everywhere in the sheath.

III. BOUNDARY CONDITIONS

From the expressions (6) giving the concentrations of the charged particles, it is easy to give a physical meaning to the parameters $C_\pm^i$. Indeed, if the potential $\phi^* - 2V_1^* a^*$ is normalized to be 0 in the plasmasphere (at $x^* = -\infty$), we deduce from (6) :

$$\phi^* (+\infty) - 2\, V_2^*\, a^* (+\infty) = \frac{1}{a_{2-}^c} \ln X$$

$$C_{\pm}^i = \frac{n_{\pm}^{*i} (+\infty)}{\rho_{\pm}^i} \; X^{\pm (a_{2\pm}^i / a_{2-}^c)} \qquad (C_{\pm}^i \neq C_-^c)$$

$$\text{where } X = \frac{n_-^{*c} (+\infty)}{C_-^c \; \rho_-^c}$$

It is seen that the potential $\phi^* - 2\, V_2^*\, a^*$ and the number densities $n^{*i}_{\pm}$ in the plasmatrough ($x^* = +\infty$) are simply related to the constants $C^i_{\pm}$. Assuming a value for C^c_-, the other constants C^c_+, C^h_-, C^h_+ and the potential at $x^* = +\infty$ are determined as functions of the densities and temperatures in the plasmatrough. For given values of the densities and temperatures at both ends of the sheath, a family of solutions can be obtained depending on the value of the free parameter C^c_- which physically determines the potential difference across the sheath.

By taking $C^c_- = 1$, the distribution of the cold electrons is a full Maxwellian and we expect therefore that the transition for the cold plasma will occur over a scale length proper to the cold ions.

Table 1 gives an example of a set of boundary conditions we have used to integrate the basic equations (8) and (9).

From table 1, it can be seen that the two types of plasma are separately neutral in the plasmasphere while it is not the case in the plasmatrough. For each type of plasma there are no variation in the temperatures across the transition. The unitary value of C^c_- corresponds to a potential difference $[\phi - 2\, aV]^{+\infty}_{-\infty}$ equal to - 5.70 V. The other constants C are found to be : $C^c_+ = 0.556 \times 10^{-4}$, $C^h_- = 14.016$ and $C^h_+ = 5.999$.

TABLE 1 : Boundary conditions .

	Plasmasphere ($x^* = -\infty$)	Plasmatrough ($x^* = +\infty$)
N^c_- (cm^{-3})	300	1
N^c_+ (cm^{-3})	300	5
N^h_- (cm^{-3})	0.5	7
N^h_+ (cm^{-3})	0.5	3
T^c_- (eV)	1	1
T^c_+ (eV)	1	1
T^h_- (KeV)	5	5
T^h_+ (KeV)	50	50

IV. NUMERICAL RESULTS

a) Some representative lengths and velocities

Before presenting the structure of the sheath it is interesting to give values for some representative lengths and velocities characterizing the problem under consideration.

It is well known that the natural unit of length (ξ_-) in a plasma sheath is the electron skin depth defined by :

$$\xi_- = \left(\frac{m_-}{\mu e^2 n_-} \right)^{1/2} = \frac{c}{\omega_p} \qquad (11)$$

It is the ratio of the speed of light (c) to the plasma frequency (ω_p). This length represents an estimation of the thickness of a boundary layer between a vacuum magnetic field and a cold plasma of zero temperature. In this case, the magnetic pressure of the field on one side is just equal to the kinetic pressure of the plasma on the other side. Then, it can be shown, (Longmire, 1963) that the electron skin depth represents the geometric mean of

the electron and ion Larmor radii (these Larmor radii refer to particles of energy equal to the corresponding thermal energy in the constant magnetic field of the vacuum side). For the cold plasma of the plasmasphere formula (11) gives $\xi_-^c(-\infty) = 307$ m.

The transition occurs near $x^* = o$ where the magnetic field has a value of 340 γ (corresponding to the dipole field at L = 4.5). Values of the bulk velocities V_1 and V_2 are taken at large distances from the sheath (at $x^* = \mp 1000$) and correspond to drift velocities equal, respectively to 1 and 1.5 times the angular velocity of the earth.

Other lengths of interest are the Larmor radii ($R_\pm^i$), which will be evaluated at $x^* = o$. Mean thermal velocities ($U_\pm^i$) are also of interest in the discussion of the stability of the transition. These values are listed in table 2.

TABLE 2 : Characteristic lengths and velocities .

$\xi_-^c(-\infty)$ (m)	$3. \times 10^2$
R_-^c (m)	10^1
R_+^c (m)	4.25×10^2
R_-^h (m)	$7. \times 10^2$
R_+^h (m)	9.5×10^4
U_-^c (m. s^{-1})	$6. \times 10^5$
U_+^c (m. s^{-1})	1.4×10^4
U_-^h (m. s^{-1})	4.2×10^7
U_+^h (m. s^{-1})	3.1×10^6

From expression (6) giving the densities, it can be seen that variations in the concentrations are linked to variations of the quantities $a_{j\pm}^{i\ 1/2}\ \gamma_\pm\ a^*$, arguments of the error function. However, the dimensioned variations of these quantities represent the inverses of the corresponding Larmor radii. Therefore, the characteristic lengths quoted in table 2 are some scale lengths characterizing the variations of the densities along the x-axis. In particular, in

the case considered here ($C^c_. = 1$, $a^c_{1\pm} = a^c_{2\pm} = 1$), the concentrations of the cold plasma decrease with the electric potential, $\phi^* - 2a^*V^*$, on which they depend exponentially and the transition will occur over a scale length comparable to the cold ion Larmor radius (425 m).

b) Structure of the sheath

Figure 2 shows the transition profile for the densities. As expected, the cold plasma (1 eV) scales according to the cold ion Larmor radius in the center of the sheath. Its density decreases from 300 particles per cm^3 to 6 particles per cm^3 for the ions and to 0.8 particle per cm^3 for the electrons over a distance equal to 7 cold electron skin depths, which represents only 2.1 km. The thickness of this transition is equal to about 5 times the cold proton Larmor radius. At the edge of the sheath, the cold plasma scales according to the hot ion Larmor radius and the asymptotic values of its densities is reached at many times the hot proton Larmor radius. The hot (5 KeV) ring electron density reaches its asymptotic values across a transition of about 10 units of length which represent 4 or 5 times the hot electron Larmor radius. As for the very hot (50 KeV) ring proton density it scales also according to its own Larmor radius and reaches its asymptotic values across a transition of about 5 times this characteristic length.

The thickness of the transition for the cold plasma should be considered as a *minimum thickness* because we did not take into account any collisional or wave-particle interactions effects which tend to broaden this boundary layer. In figure 3, we have plotted the bulk velocities $V^i_\pm$ of each species :

$$V^i_\pm = V^i_{D\pm} - V_o$$

where $V^i_{D\pm}$ are the total drift velocities :

$$V^i_{D\pm} = \pm \frac{J^i_\pm}{n^i_\pm e}$$

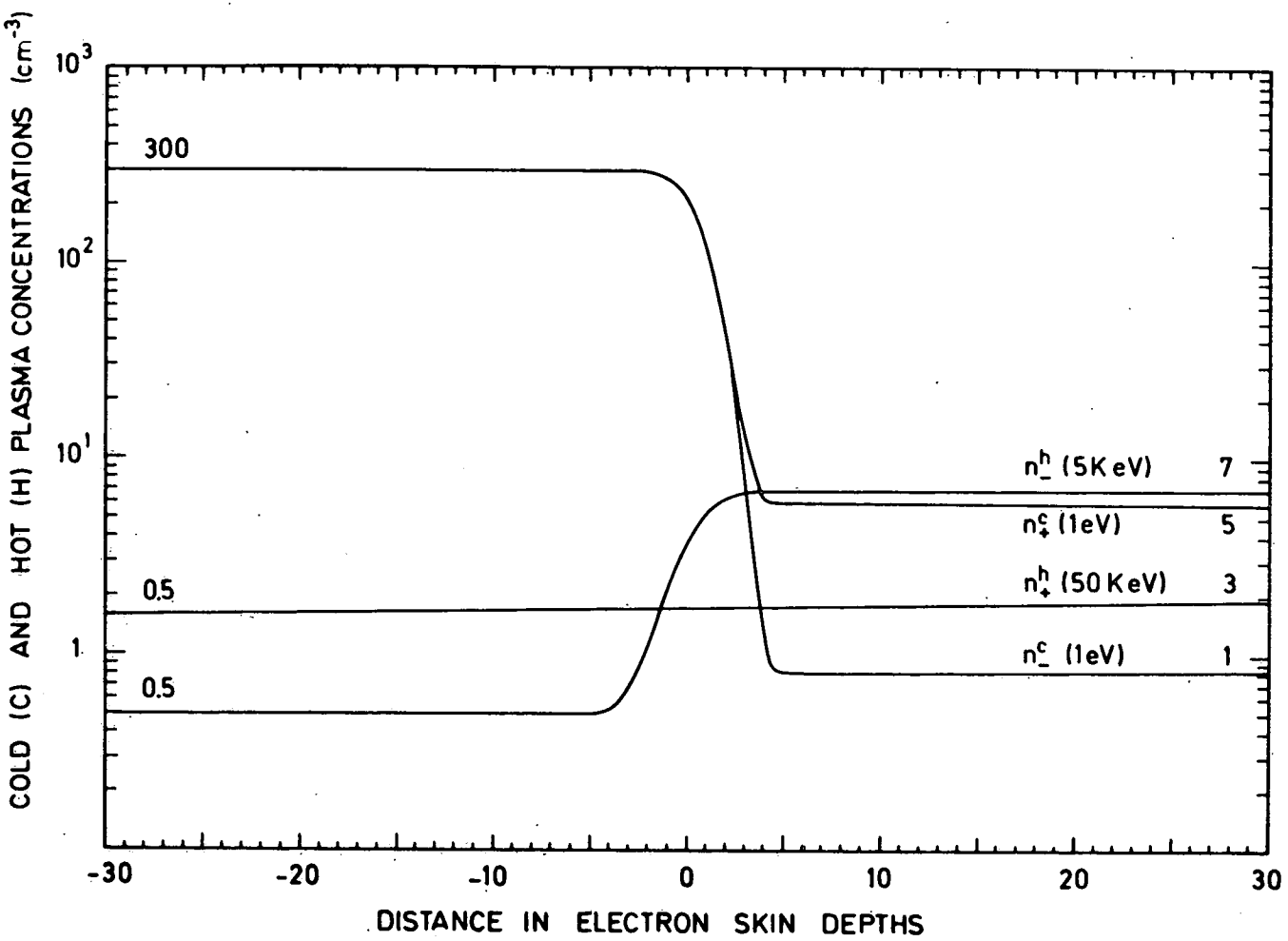

Fig. 2.- Transition profiles for the densities. The subscripts + and - are for the ions and electrons. The superscripts c and h denote respectively the cold plasma and the hot plasma. Numbers at both ends of the curves are the asymptotic values (cm^{-3}) of the densities. Numbers between parentheses are the temperatures of the corresponding species. The unit of length is the electron skin depth ξ_-^c ($-\infty$) equal to 306 m.

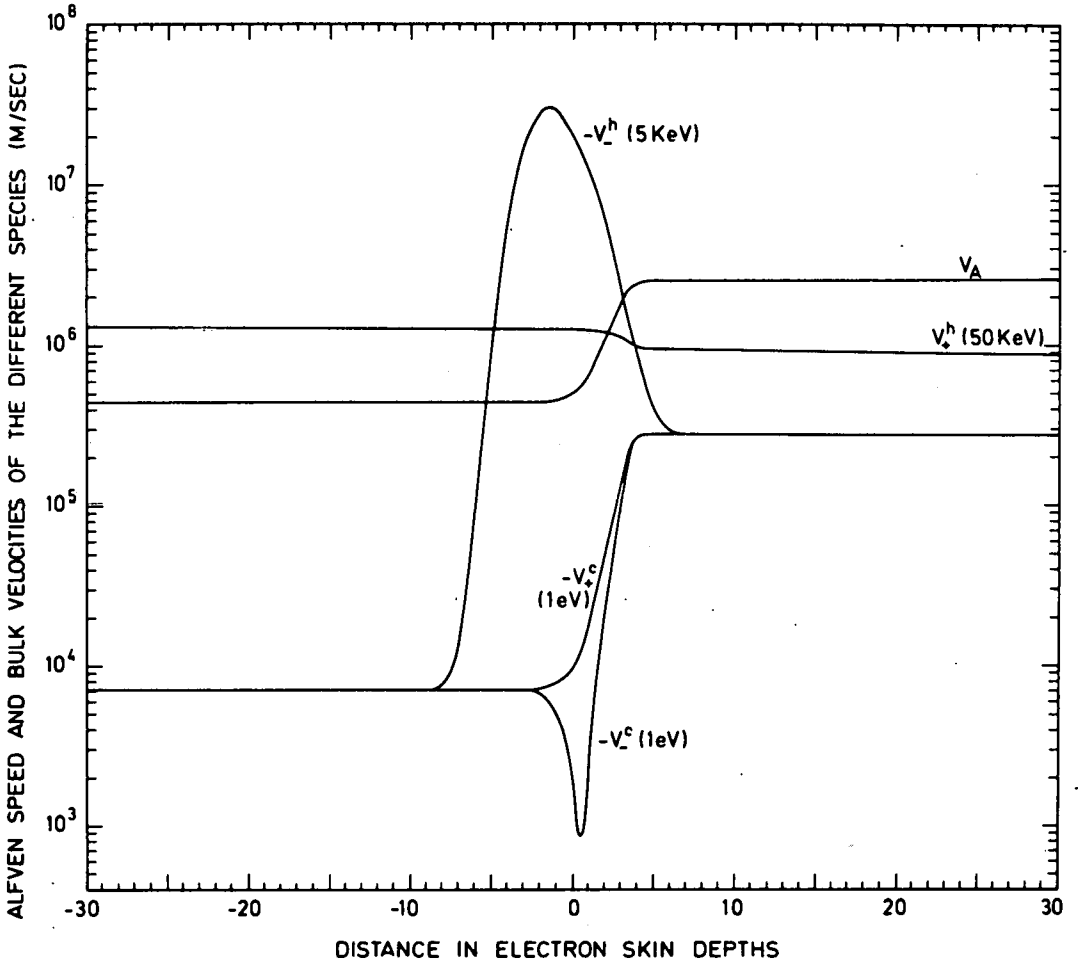

Fig. 3.- Bulk velocities $V_{\pm}^{i}$ of the different species relatively to the mass velocity. Also shown is the Alfvèn speed V_A. The superscripts c and h denote respectively the cold plasma and the hot plasma. Numbers between parentheses are the corresponding temperatures. The unit of length is the electron skin depth $\xi_-^c(-\infty)$ equal to 306 m. Thermal ions speeds for the hot and cold particles are respectively equal to 3.1×10^6 m.s^{-1} and 1.4×10^4 m.s^{-1}. An instability occurs when the relative velocity of the ions and electrons exceeds the thermal ions speed. For the cold plasma, this instability is electrostatic in nature for the relative velocity does not exceed the local Alfvèn wave speed and occurs for $1 < x^* < 4$. For the hot plasma, the relative velocity exceeds the local Alfvèn wave speed and the electromagnetic instability occurs for $-5 < x^* < 3.5$.

and V_o is the mass velocity :

$$V_o = \frac{m_- n_-^c V_{D-}^c + m_+ n_+^c V_{D+}^c + m_- n_-^h V_{D-}^h + m_+ n_+^h V_{D+}^h}{m_+ (n_+^c + n_+^h) + m_- (n_-^c + n_-^h)}$$

The Alfvèn wave speed given by

$$V_A = \frac{B}{\sqrt{\mu\rho}}$$

is also plotted for comparison.

As the relative velocity of the hot electrons and ions $V_{\pm}^h - V_-^h$ exceeds the thermal velocity of the ions ($U_+^h = 3.1 \times 10^6$ m.s^{-1}) in the transition region between $x^* \sim -5$ and $x^* \sim 3.5$, a hydrodynamic beam instability occurs (Papadopoulos, 1973). For the cold plasma the same instability is present between $x^* \sim 1$ and $x^* \sim 4$ ($U_+^c = 1.4 \times 10^4$ m.s^{-1}) but is electrostatic in nature for the relative velocity is smaller than the local Alfvèn wave speed.

Figure 4 shows the variation of the electric potential and electric field. By calculating the slope of the E-variation, it is shown that the charge neutrality approximation remains valid everywhere through the sheath. (At $x^* \sim 4$, the relative excess charge $\Delta q/q_+$ calculated by evaluating the slope $d^2\phi/dx^2$ is maximum and takes a value of 2×10^{-4}). However, it can be seen that even the small deviation from electric neutrality produces excessively large electric field. This field reaches a maximum value of 6 mV/m near $x^* \sim 3$.

Finally, the total diamagnetic current is principally due to the hot ring current particles and causes a large decrease of the magnetic field, with increasing x^*, of about 200 γ. This variation scales with a length related to the hot ion Larmor radius and takes place over a distance of several hundreds of units of length.

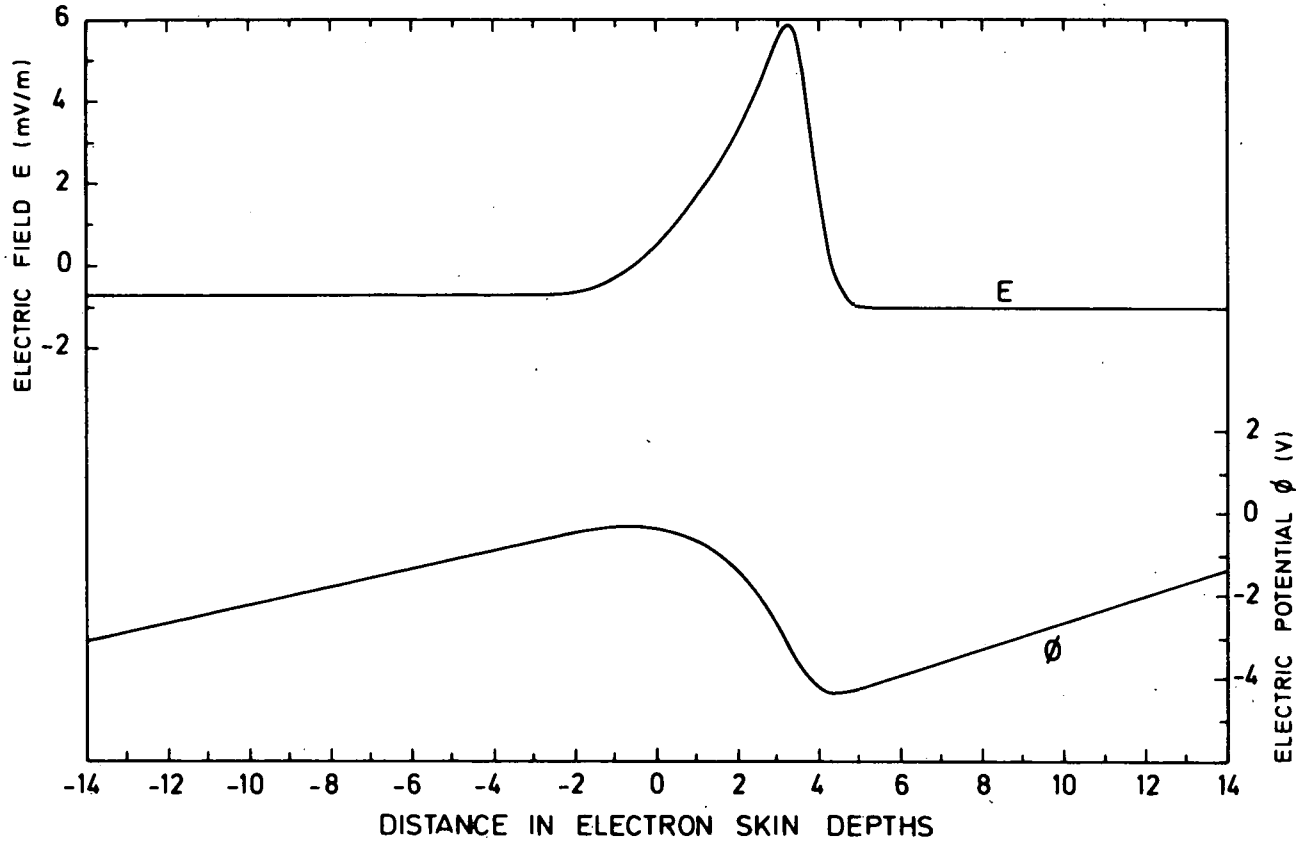

Fig. 4.- Variations of the electric field (E) and electric potential (ϕ) through the sheath. The unit of length is the electron skin depth $\xi^c_-(-\infty)$ equal to 306 m.

V. CONCLUSIONS

In this paper we have described the structure of a plasma layer, the plasmapause, separating two regions of the magnetosphere, with distinctly different properties. This microscopic description uses the Vlasov-Maxwell's equations for the charged particles and fields. Using distribution functions similar to those used by Sestero (1966) for the study of contact discontinuities in collisionless plasmas, we have computed transition profiles for the different species. For the cold plasma, the profile is ion-dominated (i.e., with negligible contribution of the electron current to the change in magnetic field). This is done by using a distribution function for the cold electrons which remains a total Maxwellian throughout the sheath. The density for the cold particles drops from 300 particles per cm^3 to a few particle per cm^3 over a distance equal to 5 times the cold ion Larmor radius. With the boundary conditions given in Section III, this transition has a thickness of 2.1 km. However in Section IV, it is shown that, in a thin region of the sheath, the cold plasma is electrostaticly unstable. This instability will destroy the steady-state transition and will lead to a broadening of the transition layer.

As the model does not take into account of any collisional effects or wave-particle interactions, the thickness of the plasmapause we calculate, must therefore be considered as a minimum thickness, although it is also possible to construct a cold electron-dominated transition (probably more strongly unstable) with a characteristic thickness of at least a cold electron Larmor radius.

The presence of the hot plasma has a great influence on the variation of the magnetic field, as it furnishes the greatest contribution to the current density. In Section IV, it is shown that the hot plasma becomes unstable near the middle of the sheath. This electromagnetic instability will in turn allow for an increase of the layer thickness.

Finally, an increase of the temperature of the cold ions in the plasmatrough ($a^c_{2+} < 1$) and the inclusion of finite integrated Pedersen and Hall conductivities would also lead to a broadening of the ideal layer discussed here.

ACKNOWLEDGEMENTS

The author is deeply grateful to Dr. J. Lemaire for his valuable comments in evaluating this paper. He is also indebted to Professor M. Nicolet for useful advices and constant encouragement.

REFERENCES

LONGMIRE, C.L., *Elementary Plasma Physics* 296 pp., Interscience, New York, 1963.

PAPADOPOULOS, K., Non thermal turbulent heating in the solar envelope, *Astrophys. J.*, **179**, 939, 1973.

SESTERO, A., Structure of plasma sheaths, *Phys. Fluids*, 7, 44, 1964.

SESTERO, A., Vlasov equation study of plasma motion across magnetic fields, *Phys. Fluids*, **9**, 2006, 1966.

100 - BIAUME, F., Détermination de la valeur absolue de l'absorption dans les bandes du système de Schumann-Runge de l'oxygène moléculaire, 1972.

101 - NICOLET, M. and W. PEETERMANS, The production of nitric oxide in the stratosphere by oxidations of nitrous oxide, 1972.

102 - VAN HEMELRIJCK, E. et H. DEBEHOGNE, Observations au Portugal de phénomènes lumineux se rapportant à une expérience de lâcher de barium dans la magnétosphère, 1972.

103 - NICOLET, M. et W. PEETERMANS, On the vertical distribution of carbon monoxide and methane in the stratosphere, 1972.

104 - KOCKARTS G., Heat baiance and thermal conduction, 1972.

105 - ACKERMAN, M. and C. MULLER, Stratospheric methane from infrared spectra, 1972.

106 - ACKERMAN, M. and C. MULLER, Stratospheric nitrogen dioxide from infrared absorption spectra, 1972.

107 - KOCKARTS, G., Absorption par l'oxygène moléculaire dans les bandes de Schumann-Runge, 1972.

108 - LEMAIRE, J. et M. SCHERER, Comportements asymptotiques d'un modèle cinétique du vent solaire, 1972.

109 - LEMAIRE, J. and M. SCHERER, Plasma sheet particle precipitation : A kinetic model, 1972.

110 - BRASSEUR, G. and S. CIESLIK, On the behavior of nitrogen oxides in the stratosphere, 1972.

111 - ACKERMAN, M. and P. SIMON, Rocket measurement of solar fluxes at 1216 Å, 1450 Å and 1710 Å, 1972.

112 - CIESLIK, S. and M. NICOLET, The aeronomic dissociation of nitric oxide, 1973.

113 - BRASSEUR, G. and M. NICOLET, Chemospheric processes of nitric oxide in the mesosphere and stratosphere, 1973.

114 - CIESLIK, S. et C. MULLER, Absorption raie par raie dans la bande fondamentale infrarouge du monoxyde d'azote, 1973.

115 - LEMAIRE, J. and M. SCHERER, Kinetic models of the solar and polar winds, 1973.

116 - NICOLET, M., La biosphère au service de l'atmosphère, 1973.

117 - BIAUME, F., Nitric acid vapor absorption cross section spectrum and its photodissociation in the stratosphere, 1973.

118 - BRASSEUR, G., Chemical kinetic in the stratosphere, 1973.

119 - KOCKARTS, G., Helium in the terrestrial atmosphere, 1973.

120 - ACKERMAN, M., J.C. FONTANELLA, D. FRIMOUT, A. GIRARD, L. GRAMONT, N. LOUISNARD, C. MULLER and D. NEVEJANS, Recent stratospheric spectra of NO and NO_2, 1973.

121 - NICOLET, M., An overview of aeronomic processes in the stratosphere and mesosphere, 1973.

122 - LEMAIRE, J., The "Roche-Limit" of ionospheric plasma and the formation of the plasmapause, 1973.

123 - SIMON, P., Balloon measurements of solar fluxes between 1960 Å and 2300 Å, 1974.

124 - ARIJS, E., Effusion of ions through small holes, 1974.

125 - NICOLET, M., Aëronomie, 1974.

126 - SIMON, P., Observation de l'absorption du rayonnement ultraviolet solaire par ballons stratosphériques, 1974.

127 - VERCHEVAL, J., Contribution à l'étude de l'atmosphère terrestre supérieure à partir de l'analyse orbitale des satellites, 1973.

128 - LEMAIRE, J. and M. SCHERER, Exospheric models of the topside ionosphere, 1974.

129 - ACKERMAN, M., Stratospheric water vapor from high resolution infrared spectra, 1974.

130 - ROTH, M., Generalized invariant for a charged particle interacting with a linearly polarized hydromagnetic plane wave, 1974.

131 - BOLIN, R.C., D. FRIMOUT and C.F. LILLIE, Absolute flux measurements in the rocket ultraviolet, 1974.

132 - MAIGNAN, M. et C. MULLER, Méthodes de calcul de spectres stratosphériques d'absorption infrarouge, 1974.

133 - ACKERMAN, M., J.C. FONTANELLA, D. FRIMOUT, A. GIRARD, N. LOUISNARD and C. MULLER, Simultaneous measurements of NO and NO_2 in the stratosphere, 1974.

134 - NICOLET, M., On the production of nitric oxide by cosmic rays in the mesosphere and stratosphere, 1974.

135 - LEMAIRE, J. and M. SCHERER, Ionosphere-plasmasheet field aligned currents and parallel electric fields, 1974.

136 - ACKERMAN, M., P. SIMON, U. von ZAHN and U. LAUX, Simultaneous upper air composition measurements by means of UV monochromator and mass spectrometer, 1974.

137 - KOCKARTS, G., Neutral atmosphere modeling, 1974.

138 - BARLIER, F., P. BAUER, C. JAECK, G. THUILLIER and G. KOCKARTS, North-South asymmetries in the thermosphere during the last maximum of the solar cycle, 1974.

139 - ROTH, M., The effects of field aligned ionization models on the electron densities and total flux tubes contents deduced by the method of whistler analysis, 1974.

140 - DA MATA, L., La transition de l'homosphère à l'hétérosphère de l'atmosphère terrestre, 1974.

141 - LEMAIRE, J. and R.J. HOCH, Stable auroral red arcs and their importance for the physics of the plasmapause region, 1975.

142 - ACKERMAN, M., NO, NO_2 and HNO_3 below 35 km in the atmosphere, 1975.

143 - LEMAIRE, J., The mechanisms of formation of the plasmapause, 1975.

144 - SCIALOM, G., C. TAIEB and G. KOCKARTS, Daytime valley in the F1 region observed by incoherent scatter, 1975.

145 - SIMON, P., Nouvelles mesures de l'ultraviolet solaire dans la stratosphère, 1975.

146 - BRASSEUR, G. et M. BERTIN, Un modèle bi-dimensionnel de la stratosphère, 1975.

147 - LEMAIRE, J. et M. SCHERER, Contribution à l'étude des ions dans l'ionosphère polaire, 1975.

148 - DEBEHOGNE, H. et E. VAN HEMELRIJCK, Etude par étoiles-tests de la réduction des clichés pris au moyen de la caméra de triangulation IAS, 1975.

149 - DEBEHOGNE, H. et F. VAN HEMELRIJCK, Méthode des moindres carrés appliquée à la réduction des clichés astrométriques, 1975.

150 - DEBEHOGNE, H. et E. VAN HEMELRIJCK, Contribution au problème de l'abérration différentielle, 1975.

151 - MULLER, C. and A.J. SAUVAL, The CO fundamental bands in the solar spectrum, 1975.

152 - VERCHEVAL, J., Un effet géomagnétique dans la thermosphère moyenne, 1975.

153 - AMAYENC, P., D. ALCAYDE and G. KOCKARTS, Solar extreme ultraviolet heating and dynamical processes in the mid-latitude thermosphere, 1975.

154 - ARIJS, E. and D. NEVEJANS, A programmable control unit for a balloon borne quadrupole mass spectrometer, 1975.

155 - VERCHEVAL, J., Variations of exospheric temperature and atmospheric composition between 150 and 1100 km in relation to the semi-annual effect, 1975.

156 - NICOLET, M., Stratospheric Ozone : An introduction to its study, 1975.

157 - WEILL, G., J. CHRISTOPHE, C. LIPPENS, M. ACKERMAN and Y. SAHAI, Stratospheric balloon observations of the southern intertropical arc of airglow in the southern american aera, 1976.

158 - ACKERMAN, M., D. FRIMOUT, M. GOTTIGNIES, C. MULLER, Stratospheric HCl from infrared spectra, 1976.

159 - NICOLET, M., Conscience scientifique face à l'environnement atmosphérique, 1976.

160 - KOCKARTS, G., Absorption and photodissociation in the Schumann-Runge bands of molecular oxygen in the terrestrial atmosphere, 1976.

161 - LEMAIRE, J., Steady state plasmapause positions deduced from McIlwain's electric field models, 1976.